The Abdus Salam International Centre for Theoretical Physics

2449-10

38th Conference of the Middle European Cooperation in Statistical Physics - MECO38

25 - 27 March 2013

Fractal Signatures in Multi-Scale Domain Morphologies

Varsha BANERJEE

Department of Physics
IIT Delhi
India

Fractal Signatures in Multi-Scale Domain Morphologies

Varsha Banerjee

Department of Physics
IIT Delhi

March 26, 2013

Outline

I. Signatures of Fractal Morphologies.

II. Random Field Ising Model and Dilute Antiferromagnets.

III. Double Phase-Separating Mixtures.

IV. Viscoelastic Phase-Separating Mixtures.

Collaborators - Gaurav Shrivastav, Siddharth Krishnamoorthy and Sanjay Puri (JNU)

I. Fractals abound in Nature

They are observed in growth profiles, colloidal aggregates, bacterial and insect colonies, dielectric breakdowns, etc.

example: aggregation of Pt atoms on a Pt(111) surface (hexagonal lattice)

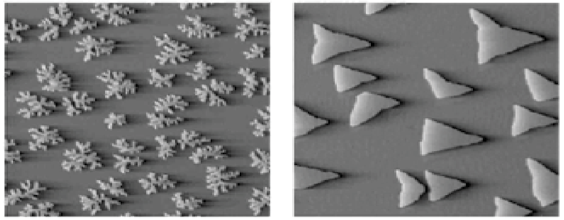

Fig. 13: *Pt island formation at temperatures $T = 300K$ (left) and $T = 400K$ (right)*
c/o T. Michely, Univ. Aachen/Germany
At low temperatures, islands resemble DLA–clusters, at higher T diffusion along edges smoothens the shape

---

Fig. 14: *Various growth or branching processes, from left to right: electrochemical deposition, mineralization pattern, * Triacontane on SiO_x,bacteria, termite colonies*

source: http://users.unim.it/bimetis/demo/dla/dla.html
and $(*)$ www.mpikg-golm.mpg.de/gf/people/riegler

Domains & interfaces are characterized by non-integer fractal dimensions.

Tools for morphology characterization

- The standard probe is the correlation function:

$$C(r) = \langle \psi(\vec{r_i})\,\psi(\vec{r_j})\rangle - \langle \psi(\vec{r_i})\rangle\langle \psi(\vec{r_j})\rangle,$$

  where $\psi(\vec{r_i})$ is an appropriate variable and $r = |\overrightarrow{r_i} - \overrightarrow{r_j}|$. The angular brackets denote an ensemble average.

- Correlation length ξ:

  Distance over which $C(r)$ decays to (say) $0.2\times$ maximum value.

Textures of domains and interfaces

$$C(r) \simeq \begin{cases} Ar^{\alpha}, & w \ll r \ll \xi, \\ Br^{\beta}, & a \ll r \ll w, \\ Gr^{\gamma}, & r \ll a. \end{cases}$$

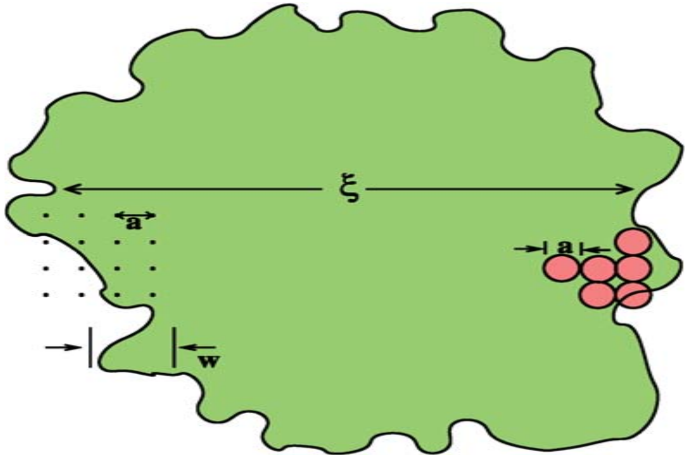

- For smooth domain, $\alpha = 1$, signifying a Porod decay.
  For fractal domain, $\alpha = d_m - d$.
- For fractal interface, $\beta = d - d_s$.
- For particles of diameter a, $\gamma = 1$ yielding a Porod decay.

(Sorensen, Aerosol Science and Technology, 2001)

Structure factor

- Small-angle scattering experiments yield the structure factor:

$$S(\vec{k}) = \int d\vec{r} e^{i\vec{k}\cdot\vec{r}} C(r),$$

where $\vec{k}$ is the wave-vector of the scattered beam.

$$S(k) \simeq \begin{cases} \tilde{A} k^{-(d+\alpha)}, & \xi^{-1} \ll k \ll w^{-1}, \\ \tilde{B} k^{-(d+\beta)}, & w^{-1} \ll k \ll a^{-1}, \\ \tilde{G} k^{-(d+\gamma)}, & a^{-1} \ll k. \end{cases}$$

- The Porod decay $k^{-(d+1)}$ indicates smooth domains or interfaces.

  $k^{-(d\pm\theta)}$ indicates a fractal structure in the domains or interfaces.

II. Random Field Ising Model

- Energy function

$$E = -J \sum_{\langle ij \rangle} \sigma_i \sigma_j - \sum_{i=1}^{N} h_i \sigma_i, \quad \sigma_i = \pm 1.$$

  - The interaction $J > 0$ prefers a magnetized structure.
  - The (disordering) random fields $\{h_i\}$ are drawn from:

$$p(h_i) \quad = \quad \frac{1}{\sqrt{2\pi}\Delta} e^{(-{h_i}^2/2\Delta^2)}.$$

- Archetypal example of a system with disorder and frustration.
- Approach to the GS is difficult due to the complex energy landscape.
- Exact ground states of the RFIM can be obtained by graph-cut (max-flow/min-cut) algorithms.

(Angles d'Auriac, Preissmann, Rammal, J. Phys. (France) Lett. 1985)

GS of the RFIM

- By computing the Binder cumulant, $\Delta_c(T = 0) \simeq 2.278 \pm 0.002$.
- Emergence of domains of size ξ as Δ reduced from $\Delta = \infty$.
- $\xi \to \infty$ as $\Delta \to \Delta_c^+$.

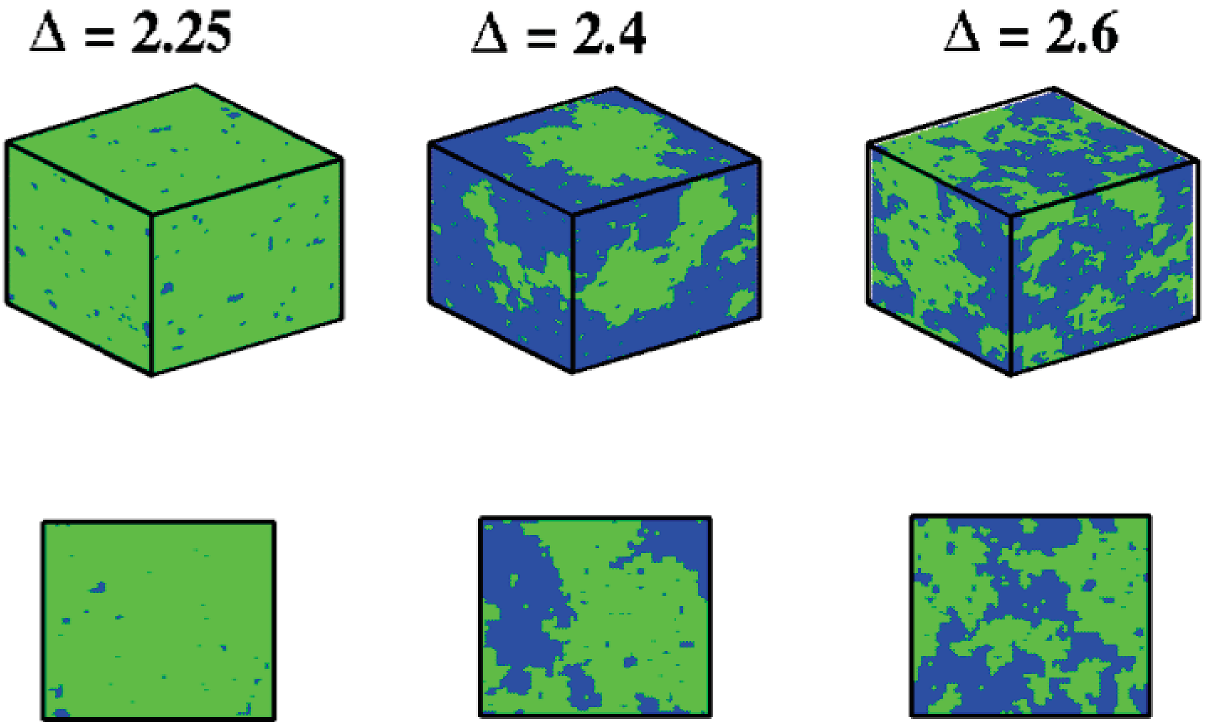

$T = 0$; $L = 256$ with pbc; 100 sets of $\{h_i\}$ for each Δ.

(Shrivastav, Krishnamoorthy, VB, Puri, EPL, 2011)

Scaling of $C(r, \Delta)$

- $C(r, \Delta)$ vs. r/ξ, $\Delta > \Delta_c$:

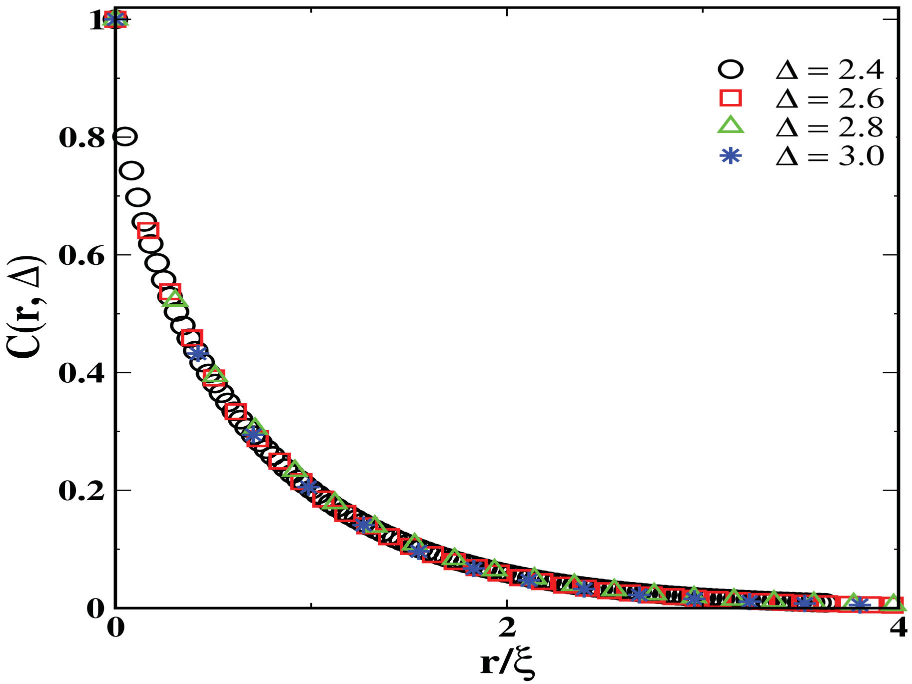

- System characterized by a single length scale ξ.
- Morphologies are scale invariant with respect to change in Δ.

(Shrivastav, Krishnamoorthy, VB, Puri, EPL, 2011)

$C(r, \Delta)$ at small-r

- Exhibits a cusp-singularity:
  $C(r, \Delta) \simeq 1 - A(r/\xi)^{\beta}, \; r \ll w$
  with $\beta \simeq 0.5$

- The cusp-exponent β quantifies interfacial roughness.

- Interfaces are self-affine fractals:
  $d_s = d - \beta$.
  (Wong & Bray, PRL, PRB, 1988; Barma, EPJB, 2008)

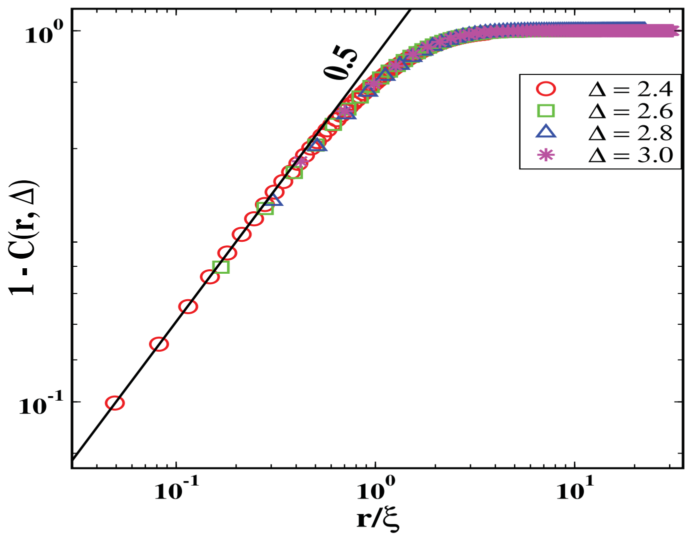

(Shrivastav, Krishnamoorthy, VB, Puri, EPL, 2011)

- In the paramagnetic phase, $d_s \simeq 2.5$.

A similar cusp has also been reported in the context of *fluctuation dominated phase separation.* **(Das & Barma, PRL, 2000; Mishra & Ramaswamy, PRL, 2006)**

Larger-r behavior of $C(r, \Delta)$

$$C(r, \Delta) \simeq B(r/\xi), \quad w \ll r \ll \xi.$$

The linear decay is the Porod law characteristic of scattering from sharp interfaces in inhomogeneous systems. **(Oono & Puri, Mod.Phy.Lett., 1988)**

- "a" is the lattice spacing.
- No systematic structure for $r \sim a$.
- Cusp singularity for $a \ll r \ll w$;
- Porod decay for $w \ll r \ll \xi$.

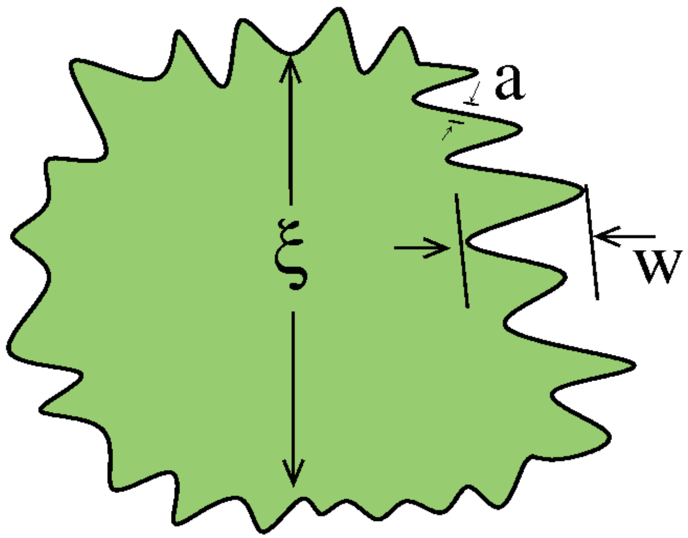

Implications for $S(k,\Delta)$

Asymptotic power law decay for $k \ll a^{-1}$:

$$S(k,\Delta) \sim \tilde{A}(\xi k)^{-(d+\beta)} + \tilde{B}(\xi k)^{-(d+1)}$$

(Bale & Schmidt, PRL, 1984; Wong & Bray, PRL, 1988)

- Porod regime at intermediate values of k: $S(k,\Delta) \sim k^{-(d+1)}$.
- Asymptotic cusp regime: $S(k,\Delta) \sim k^{-(d+\beta)}$, $\beta \simeq 0.5$.
- Cross-over momentum $k_c(\Delta) \sim \xi^{-1}$

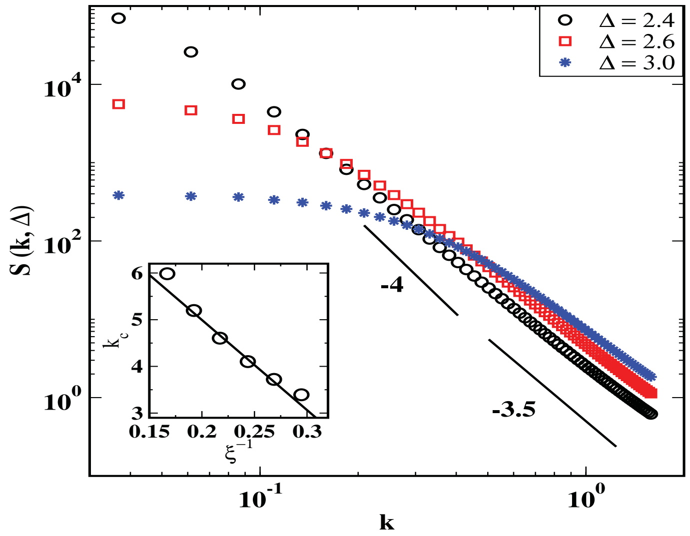

(Shrivastav, Krishnamoorthy, VB, Puri, EPL, 2011)

Crossover due to interfacial roughening caused by quenched disorder.

- Diluted Antiferromagnets (DAFs) in a uniform field are realizations of the RFIM. **(Fishman & Aharony, J. Phys. C, 1978)**

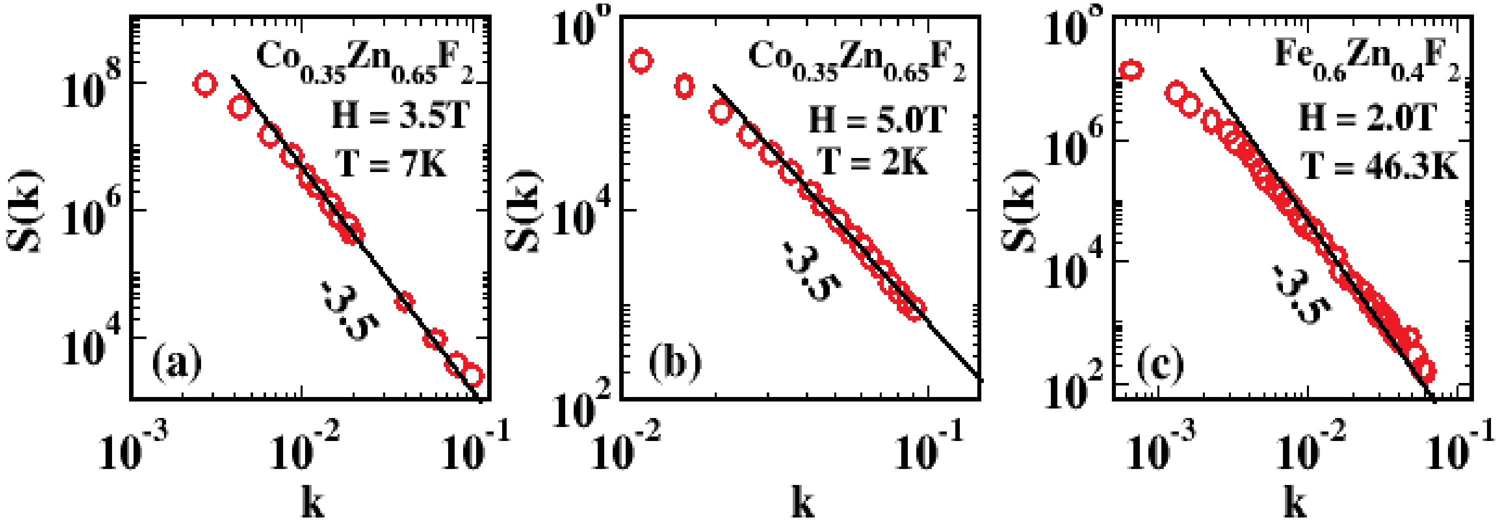

Scattering data from DAFs by Belanger, *et al.*, PRB, 1985.

- All three data exhibit an asymptotic cusp regime $[S(k) \sim k^{-3.5}]$. **(Shrivastav, VB, Puri)**

III. Double phase-separating symmetric binary mixture

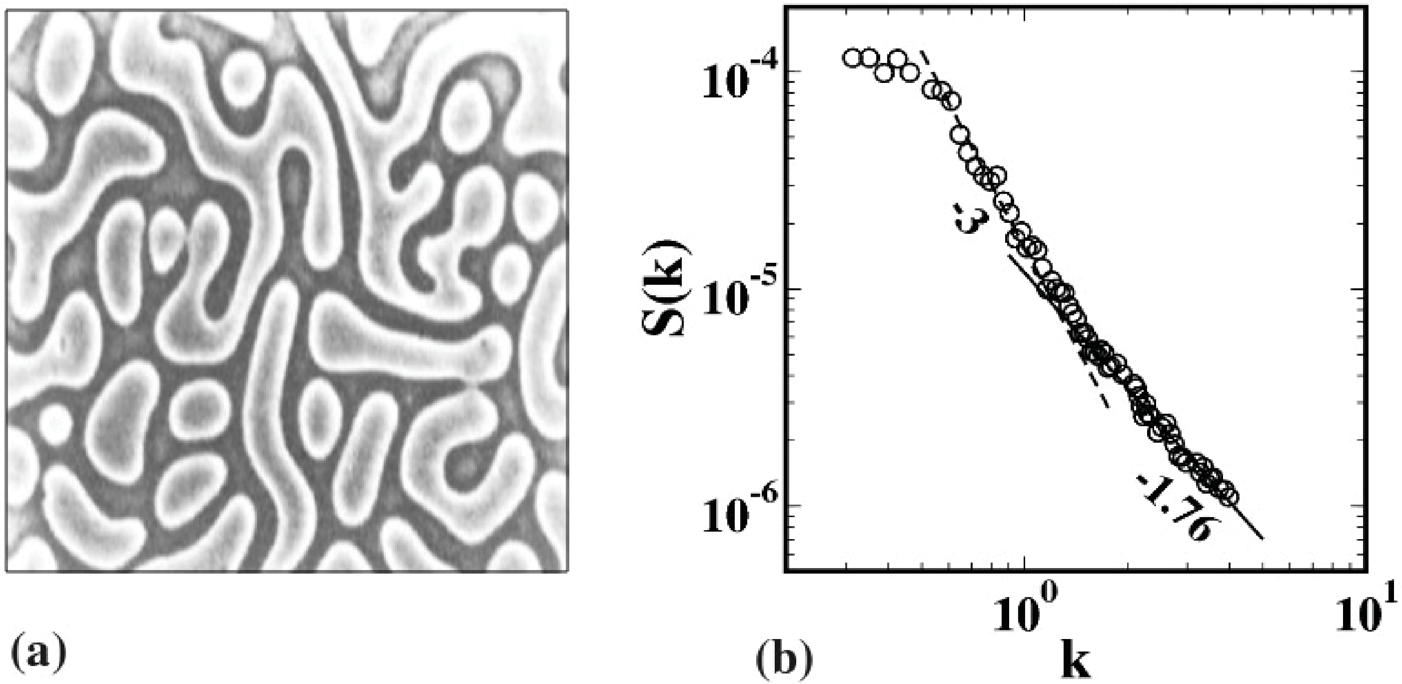

- Droplet-in-droplet morphology of an ordering mixture of poly-vinyl-methyl-ether and water in $d = 2$. **(Tanaka, PRL, 1994).**
- Corresponding $S(k)$ vs. k exhibiting a cross-over from a Porod regime $[S(k) \sim k^{-3}]$ to a mass fractal regime $[S(k) \sim k^{-1.76}]$. **(Shrivastav, VB, Puri)**

Droplet-in-droplet morphology in DPS

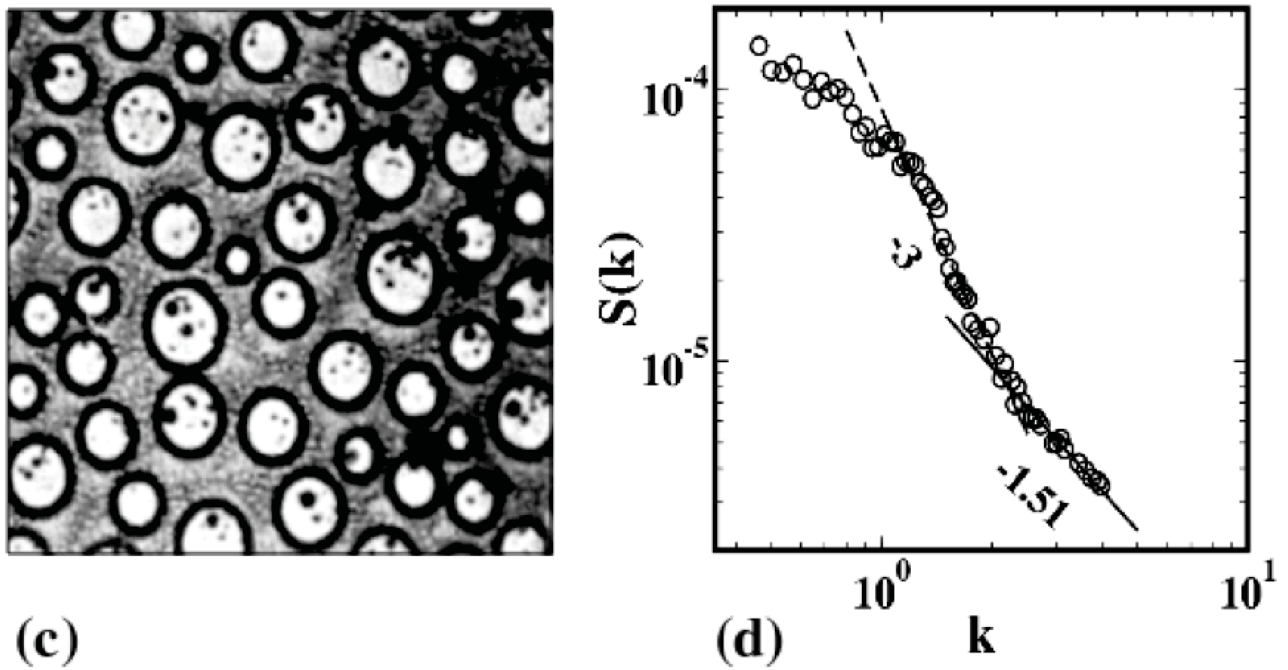

- Microstructure of an ordering mixture of ϵ-caprolactone and styrene oligomers in $d = 2$. **(Tanaka, PRL, 1994).**
- Corresponding $S(k)$ vs. k exhibits a cross-over from a Porod regime $[S(k) \sim k^{-3}]$ to a mass fractal regime $[S(k) \sim k^{-1.51}]$.
  (Shrivastav, VB, Puri)

IV. Viscoelastic phase separation in asymmetric mixtures

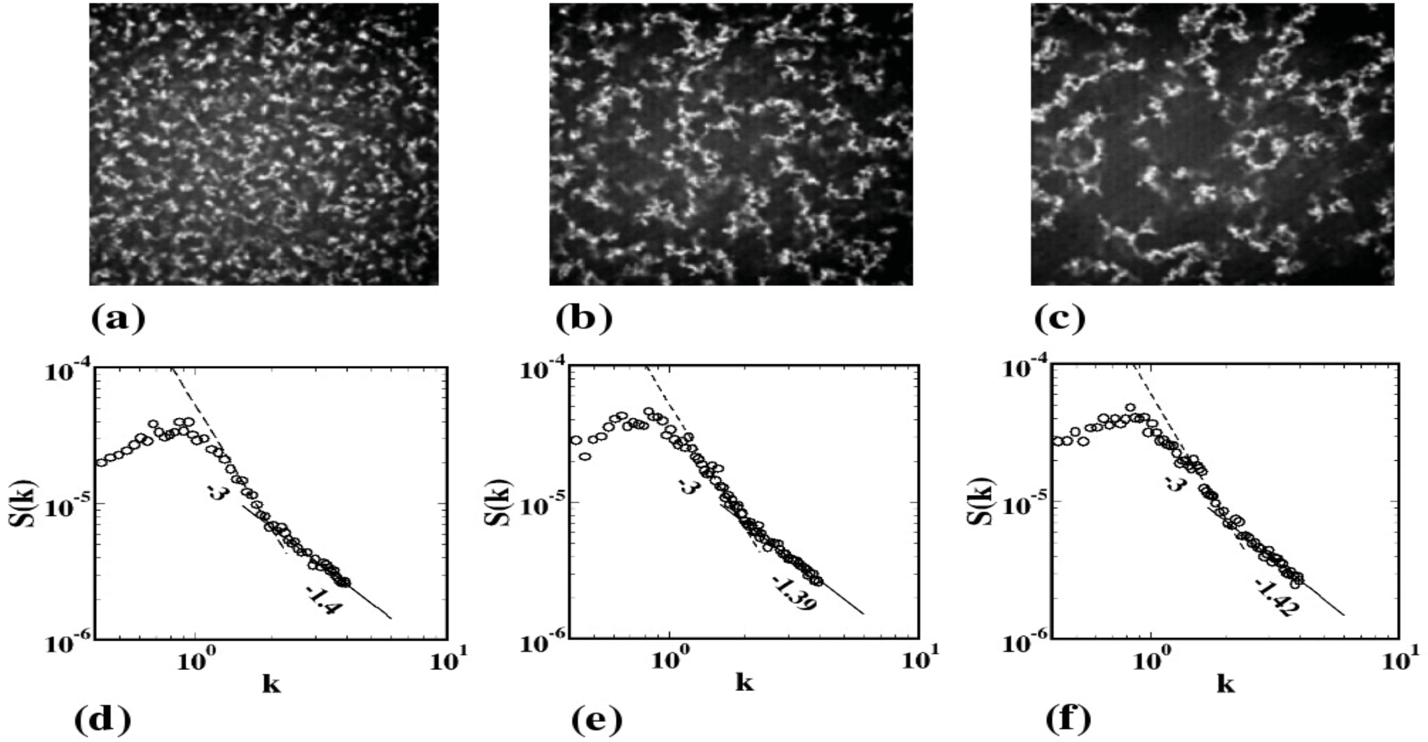

- VPS in a polystyrene and aqueous NaCl suspension for $t = 270$ s, 900 s and 3600 s. **(Tanaka, J Phys. Condens. Matter, 2005; PRL, 2005; 2011).**
- Smooth domains of smaller and faster (liquid) particles separated by thick (mass) fractal strings of larger and slower (colloidal) particles.

(Shrivastav, VB, Puri)

Summary

- The signature of fractal domains and interfaces is a power-law decay with non-integer exponents in $C(r)$ and $S(k)$.

- The power yields the fractal dimension of the underlying geometry, and the law holds over length scales which can probe this geometry.

- Smooth morphologies are characterized by the Porod law.

- Our re-analysis of scattering data from (i) dilute antiferromagnets, (ii) double phase-separating binary mixtures and (iii) viscoelastic phase-separating asymmetric binary mixtures reveals morphologies that are smooth on some length scales and fractal on others.

- The behaviors of $C(r)$ vs. r and $S(k)$ vs. k are therefore characterized by cross-overs from one form to another.

- The cross-over points are easy to calculate and are related to the natural length scales of the multi-scale morphologies.

GS by Standard Procedures

- Metropolis Algorithm, Simulated Annealing, Cluster Algorithm, etc.
- Involve only one or $O(1)$ spin-flip at a time.
- Convergence time to the global minimum is non-polynomial in N.
- System then opts for a local minimum which could be arbitrarily far from the global minimum.
- The local minimum may not convey any of the global properties encoded in the energy.
- Further, possibility of escape to the global minimum is small.

“Max-Flow/Min-Cut” or “Graph Cut” Methods

A specialized graph for the energy function is constructed such that the cheapest cut on the graph minimizes energy either globally or locally.

- A graph $\mathcal{G} = (\mathcal{V}, \mathcal{E})$ consisting of vertices $\mathcal{V}$ and edges $\mathcal{E}$ that connect then.
- An edge ij joining vertices i and j is assigned a weight V_{ij}.
- A cut C is a partition of the vertices $\mathcal{V}$ into two sets $\mathcal{R}$ and $\mathcal{Q}$.
- Any edge $ij \in \mathcal{E}$ with $i \in \mathcal{R}$ and $j \in \mathcal{Q}$ (or vice-versa) is a cut edge.
- The cost of a cut is the sum of weights of the cut edges.
- The min-cut problem is to find the cut with the smallest cost.

The Graph Construction

- A standard energy function:

$$E(\{s_i\}) = \sum_{\{ij\}\in\mathcal{N}} V_{ij}(s_i, s_j) + \sum_i D_i(s_i), \quad s_i \in \mathcal{L} = (\alpha, \beta, ..., \gamma).$$

- Two-terminal graph ($s_i = \alpha, \beta$):

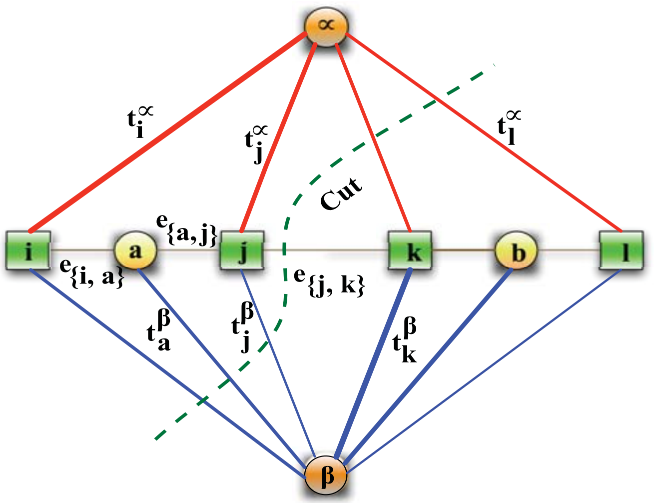

(Boykov & Kolmogorov , IEEE PAMI, 2004)

Edge	Weight	For
t_i^{β}	∞	$i \in \mathcal{R}_\alpha$
t_i^{β}	$D_i(s_i)$	$i \notin \mathcal{R}_\alpha$
t_i^{α}	$D_i(\alpha)$	$i \in \mathcal{R}_\alpha$
$e_{\{i,a\}}$	$V(s_{i,\alpha})$	$\{i,j\} \in \mathcal{N}, s_i \neq s_j$
$e_{\{a,j\}}$	$V(\alpha, s_j)$	
t_a^{β}	$V(s_i, s_j)$	

The Global Minimum

- Exact min-cut can be found in polynomial time if
  1. E is quadratic,
  2. s_i's are binary (0 or 1 say),
  3. interactions satisfy the regularity condition:

$$V_{ij}(0,0) + V_{ij}(1,1) \leq V_{ij}(1,0) + V_{ij}(0,1).$$

(Picard, Ratliff, Networks, 1975; Papadimitriou, Steiglitz, Combinatorial Optimization, 1982)

- $n_i = (1 + \sigma_i)/2$ transforms $\sigma_i = \pm 1$ to $n_i = 0, 1$.

- In physical systems, 3 corresponds to interactions $J_{ij} > 0$.

- Exact ground states of the RFIM are assured by min-cut algorithms.

(d'Auriac, Preissmann, Rammal, J. Phys. (France) Lett. 1985)

Boykov-Kolmogorov Method (BKM)

1. Start with an arbitrary labeling s.
2. Set success $:= 0$
3. For each label $s_i \in \{0, 1\}$:
   3.1 Find $\hat{s} = \arg\min E(s')$ among s' via graph cuts
   3.2 If $E(\hat{s}) < E(s)$, set $s := \hat{s}$ and success $:= 1$
4. If sucess $= 1$ go to 2
5. Return s

The convergence time to the global minimum is $O(N)$.

(Boykov & Kolmogorov , IEEE Transactions on PAMI, 2004)

Details of Numerics

- Boykov-Kolmogorov Method (BKM). **(Boykov & Kolmogorov , IEEE PAMI, 2004)**
- The convergence time to the global minimum is $O(N)$.
- $T = 0$; L^3 ($L \leq 256$) with pbc; 100 sets of $\{h_i\}$ for each Δ.
- Initial configuration a random mix of $\sigma_i = \pm 1$.
- The BKM yields a 99% overlap with the GS in the first iteration!
- (A mild "critical slowing down" observed as $\Delta \to \Delta_c$.)
- Energy per spin in the GS $\simeq$ -3.05 (BKM)
  $\simeq$ -2.69 (MC)

GS of the Ising Model

- $\Delta = 0$; $\xi \to \infty$ as $T \to T_c^+$; $T_c = 4.5103$.
- Equilibrium MC snapshot (64^3) at $T = 4.515$:

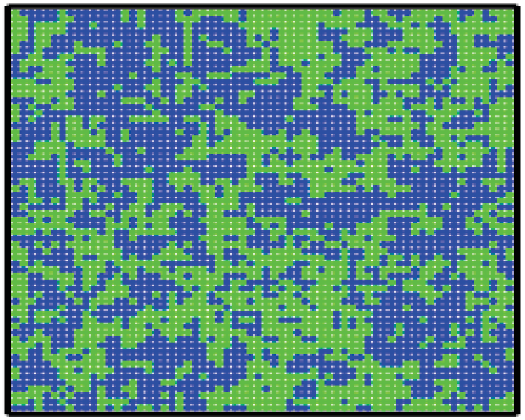

- Morphology is not as compact or well-defined.
- Morphology in the RFIM is well-defined even in the absence of coexisting phases.

Correlation Exponent ν

Plot of $\xi(\delta, L)$ vs. δ, where $\delta = (\Delta - \Delta_c)/\Delta_c$:

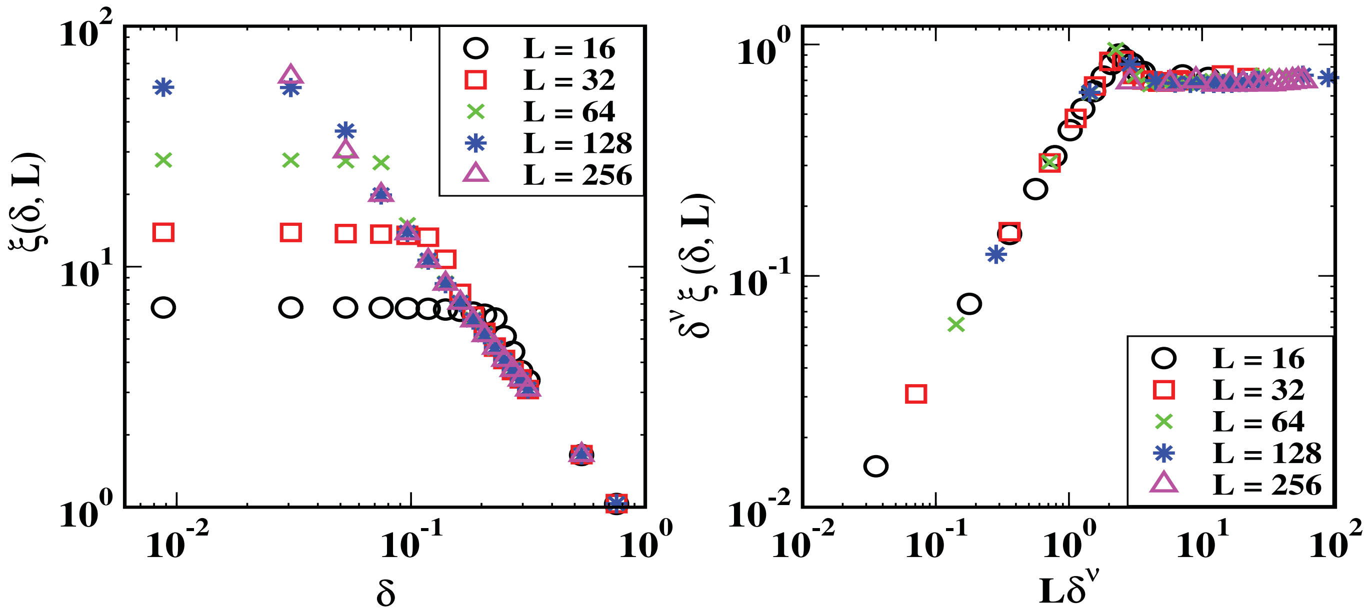

(GPS, SK, VB & SP, EPL, 2011)

- $\xi \sim \delta^{-\nu}$ when $\delta \to 0^+$ (limited by L).
- Finite-size scaling ansatz: $\xi(\delta, L) = \delta^{-\nu} f(L\delta^{\nu})$.
- $\nu = 1.308 \pm 0.005$

(1.4 ± 0.2 **Rieger & Young, J. Phys. A, 1993;** 1.37 ± 0.09**, Middleton & Fisher, PRB, 2001).**

$C(r, \Delta)$ at small-r

- Scaling function exhibits a *cusp-singularity:* $C(r, \Delta) \simeq 1 - A(r/\xi)^{\beta} + \cdots$
- The cusp-exponent β quantifies *interfacial roughness.*
- Interfaces are *self-affine fractals*: $d_s = d - \beta$.

  (Wong & Bray, PRL, PRB, 1988; Barma, EPJB, 2008)
- In the ferromagnetic phase ($\Delta \lesssim \Delta_c$), $\beta_{\text{ferro}} \simeq 0.66$; $d_s \simeq 2.34$.
- In the paramagnetic phase ($\Delta > \Delta_c$), $\beta_{\text{para}} \simeq 0.5$; $d_s \simeq 2.5$.

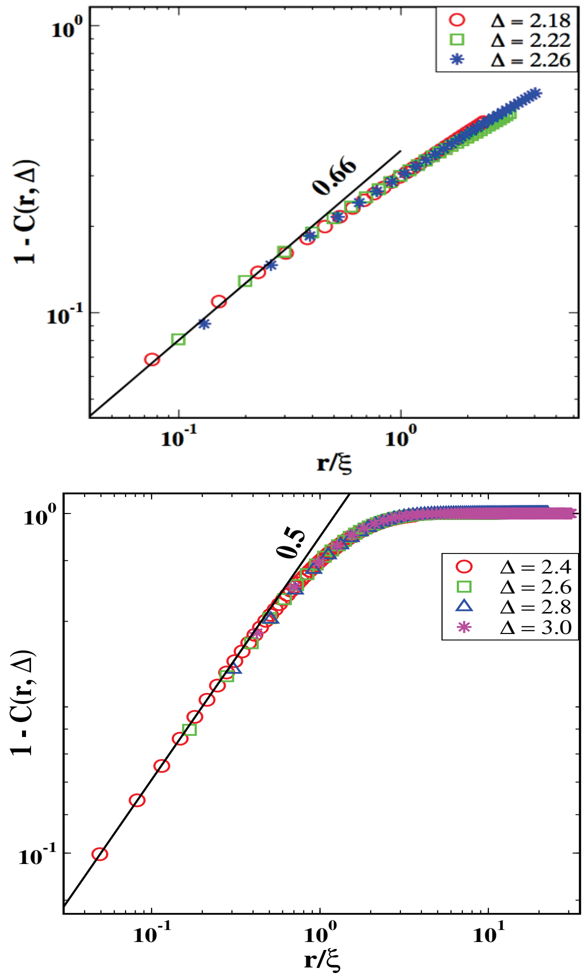

(GPS, SK, VB & SP, EPL, 2011)

Related comments

- The value $d_s \simeq 2.34$ in the ferromagnetic phase is consistent with analytical predictions. **(Imry & Ma, PRL, 1976; Halpin-Healy, PRA, 1990)**
- The paramagnetic phase of the $d = 3$ RFIM was shown to exhibit percolation type of order. **(Alava, et al., PRB, 2002; Ji & Robbins, PRB, 1992)**
- The spanning cluster in $d = 3$ percolation has the fractal dimension of $d_s \simeq 2.5$. **(Stauffer and Aharony, 1992)**
- Cusp-singularity has also been reported in fluctuation dominated phase separation:
  - Steady-state distribution of particles on a fluctuating surface. **(Das & Barma, PRL, 2000)**
  - Density correlation of ordered (active) nematics. **(Mishra & Ramaswamy, PRL, 2006)**
  - In both cases, interfaces are fuzzy or ill-defined.

Fractal dimension

- Regular objects : $M \sim R^d$, where d is the Euclidean dimension.
- Surface fractals: $S \sim R^{d_s}$, where d_s is the surface fractal dimension and $d - 1 \leq d_s < d$.

  Interfaces generated in fluid flows, burning wavefronts, pinning of flux lines, deposition processes, etc.
- Mass fractals: $M \sim R^{d_m}$, where d_m is the mass fractal dimension and $1 \leq d_m < d$.

  DLA clusters, bacterial colonies, colloidal aggregates, etc .
  Mass fractals are often bounded by surface fractals.

Usual quantities of interest are radius of gyration, roughness exponents, fractal dimensions, etc. of domains and interfaces.

Multi-scale domain morphologies

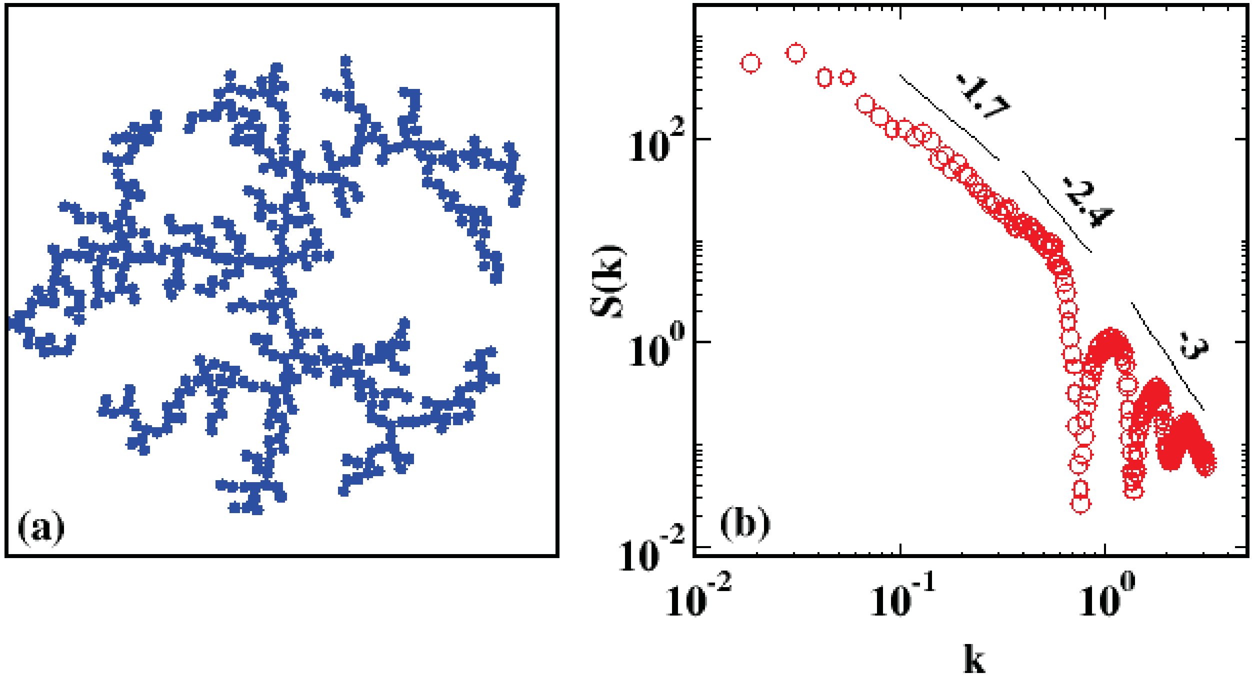

(a)

Diffusion limited aggregation (DLA) cluster created by spherical particles of size $a = 10$ in units of the lattice spacing. (b) Structure factor, $S(k)$ vs. k, for the DLA cluster in (a). The straight lines denote the mass fractal regime [$S(k) \sim k^{-d_m}$ with $d_m = 1.71$; the surface fractal regime [$S(k) \sim k^{-(2d-d_s)}$ with $d_s = 1.6$; and the Porod regime [$S(k) \sim k^{-(d+1)}$].